Transition to weak generalized synchrony in chaotically driven flows

Thounaojam Umeshkanta Singh, Haider Hasan Jafri, and Ramakrishna Ramaswamy
School of Physical Sciences, Jawaharlal Nehru University, New Delhi 110 067, India
(Received 18 July 2009; revised manuscript received 4 November 2009; published 14 January 2010)

We study regimes of strong and weak *generalized* synchronization in chaotically forced nonlinear flows. The transition between these dynamical states can occur via a number of different routes, and here we examine the onset of weak generalized synchrony through intermittency and blowout bifurcations. The quantitative characterization of this dynamical transition is facilitated by measures that have been developed for the study of strange nonchaotic motion. Weak and strong generalized synchronous motion show contrasting sensitivity to parametric variation and have distinct distributions of finite-time Lyapunov exponents.

DOI: 10.1103/PhysRevE.81.016208 PACS number(s): 05.45.Df, 05.45.Gg, 05.45.Xt

I. INTRODUCTION

Over the past few decades the study of driven nonlinear systems has revealed a number of new dynamical phenomena, and this has made the design and control of a wide variety of different dynamical behaviors possible [1,2]. Periodic driving is a widely studied case, but other forms of forcing have also been explored. One effect of driving has been stabilization, when chaotic dynamics is made nonchaotic under the influence of an external force. The most unusual instance of such transformation occurs with a quasiperiodic drive, when strange nonchaotic attractors (SNAs) [3] are created. These are a novel class of attractors that are so far unknown in unforced systems.

Another direction of research has explored synchronized entrainment of chaotic motion in coupled nonlinear dynamical systems [2]. In a sense this also involves forcing one dynamical system by another: trajectories of the response system synchronize with those of the drive, resulting in effective stabilization. Depending on the coupling and the nature of the systems, there can be a variety of forms of synchrony, and these have been discussed in detail in the recent literature [1].

Consider the "drive-response" system

$$\frac{d\mathbf{x}}{dt} = F(\mathbf{x}, \mathbf{u}, \alpha), \tag{1}$$

$$\frac{d\mathbf{u}}{dt} = G(\mathbf{u}, \beta), \tag{2}$$

where $\mathbf{x} \in \mathbb{R}^n$ and $\mathbf{u} \in \mathbb{R}^m$ are the dynamical variables of the response and drive systems respectively. The vector fields F and G are taken to be continuous and differentiable, and α and β represent control parameters. The coupled system has $n+m$ Lyapunov exponents. Given the skew-product structure the m exponents of the drive denoted by $\lambda_i^u, i=1,\ldots,m$ are unaffected by the coupling, while the remaining n exponents $\lambda_i^x, i=1,\ldots,n$ correspond to the response subsystem and are *conditional* Lyapunov exponents (CLEs).

If the drive and the response are identical, then it is well known that complete synchronization (CS) can occur [2]. However, when the drive and response are distinct, for suitable form of the coupling there is the possibility of *generalized* synchronization (GS) [4], when the state of the response system is *uniquely* dependent on the drive. An understanding of how synchronization comes about in such general settings—and indeed, the nature of synchrony between dissimilar systems—is still incomplete although numerous instances have been characterized.

In a technical sense, generalized synchronization results when the subsystem Lyapunov exponents, the λ_i^x's are nonpositive: then different trajectories of the response system can coalesce [2]. The dynamics of the response is then stable and there is an attracting invariant set which is a graph $\Phi:\mathbf{u}\to\mathbf{x}$. Since this invariant set is attracting, perturbed trajectories return to it asymptotically at an exponential rate. Although properly speaking this limit set is not a global attractor (since there is dependence on the initial conditions of the drive) this is indeed a case of generalized synchrony, and it implies the existence of a unique functional dependence, $\mathbf{x}=\Phi[\mathbf{u}]$ [4]. However, distinction should be made between the cases of the function Φ being smooth and differentiable [5,6], or not: these are known as strong and weak GS respectively.

In the present paper, we study driven flows where both the drive and the response are nonlinear oscillators. Our motivation is to analyze the state of generalized synchrony, and in particular to examine the transition from strong to weak GS. We have recently shown in studies of driven mappings that there are transitions to weak GS [7] that parallel analogous routes to chaos [8] or routes to the creation of SNAs [9] in quasiperiodically forced nonlinear systems. Here we study transitions to a state of weak generalized synchronization via intermittency as well as via a blowout bifurcation.

We examine quantitative characterizations of this dynamical transition by adapting tools that were originally introduced in the study of strange nonchaotic dynamics such as parameter sensitivity exponents. Similar measures can be useful in characterizing the transitions between strong and weak generalized synchronization, as well as the disappearance of weak GS, namely the transition from weak GS to a state of no generalized synchrony. We also use other quantitative measures such as the distribution of local Lyapunov exponents to examine the various dynamical transitions.

The phenomenon of generalized synchronization has a wide range of applicability. For instances, in the context of time-series analysis, the stabilization of recursive filters has been an important issue of practical importance [10,11] to

ensure that measurable quantities of the drive reconstructed from the filter output does not change the properties of the original drive [12]. From a technological point of view, generalized synchronization of aperiodic trajectories suggest applications in secure communications [13] and chaotic masking [14]. Chaotic motion being ubiquitous in nature, the entrainment of one system as a consequence of being driven by another can be a common method of dynamical control in physiological processes [15], neuronal systems [16], ecological systems [17], and financial markets [18], for instance. The analysis of generalized synchrony is thus of considerable interest.

The organization of this paper is as follows. As drive we take a Rössler oscillator and as response we consider two model nonlinear dynamical systems that have experimental realizations as well. In Sec. II we examine the driven Duffing oscillator and study the transition to weak GS from strong GS through intermittency. We further study a different driven nonlinear oscillator that makes this transition through a blowout bifurcation. The transition from weak synchrony to asynchrony is discussed in Sec. III, while characterization of the dynamics and the geometry of the various limit sets is discussed in Sec. IV. The paper concludes with a discussion and summary in Sec. V.

II. TRANSITIONS TO WEAK GS

We exploit the parallels that were noted in our earlier work between quasiperiodic and chaotic driving [7] to observe that when a situation of strong generalized synchronization obtains, the existence of a smooth implicit function Φ is analogous to the case of a nonfractal nonchaotic attractor. Similarly, when there is weak generalized synchronization, Φ is nonsmooth, analogous to a strange nonchaotic attractor.

The chaotic drive that we use in the present work is the Rössler oscillator

$$\frac{du}{dt} = (-v - w)f,$$

$$\frac{dv}{dt} = (u + av)f,$$

$$\frac{dw}{dt} = [b + w(u - c)]f, \tag{3}$$

with parameters $a=b=0.2$ and the factor f is a scaling parameter that is introduced in order to have some flexibility in adjusting the natural frequency of the chaotic oscillator. Specifically, we use the output signal $u(t)$ to drive the response.

A. Intermittency

The response system that we study first is a forced Duffing oscillator which is given by the following dynamical equations,

$$\frac{dx}{dt} = y,$$

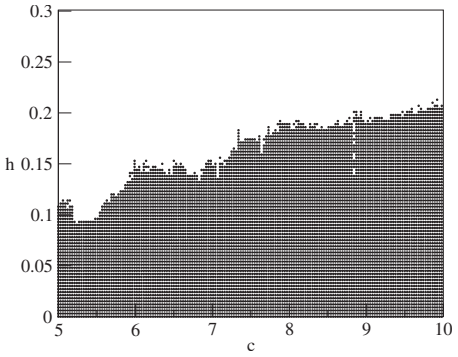

FIG. 1. Schematic phase diagram of driven Duffing oscillator Eq. (5) in the parameter space: white corresponds to regions of GS where dynamics are stabilized and black corresponds to regions of asynchrony where dynamics is chaotic.

$$\frac{dy}{dt} = -hy + x - x^3 + Ax\cos\theta,$$

$$\frac{d\theta}{dt} = 1. \tag{4}$$

Note that for $A=0$, this is passive Duffing oscillator, but for nonzero A, the system is known to display a variety of dynamics including limit cycles and chaotic behaviors.

We subject this oscillator to external driving by the Rössler oscillator (with time scale parameter in Eq. (3) is taken to be $f=1.49$); the above equation for dy/dt is thus modified as

$$\frac{dy}{dt} = -hy + x - x^3 + Ax\cos\theta + Aa_r ux. \tag{5}$$

The natural frequency of the drive and the amplitude of the signal u can be adjusted by varying the parameters f and c. Recall that the case of a sinusoidal $u(t)$ has been studied earlier in the context of transitions to SNAs [19–21].

Figure 1 shows the phase diagram of the driven Duffing oscillator Eq. (5) as a function of the parameters c in the drive equations of motion and h in the response, keeping $A=0.15$ and $a_r=0.125$. Regions in white (black) represent the dynamical state of generalized synchrony (asynchrony), namely, the response conditional Lyapunov exponent is negative (positive). To study the dynamical behavior of the drive as well as the response, we focus on the $h=0.2$ line in this phase diagram.

Figure 2 shows the variation of largest Lyapunov exponents (LEs) of the drive Eq. (3) and response Eq. (5). In a small window, we find multistability, with two coexisting attractors [22] and this region is shaded in the figure. The Rössler system shows a variety of dynamical regimes as the parameter c is varied: chaotic dynamics for parameters where LEs are positive and regular dynamics where LEs are zero. P_1, P_2, P_3, and P_4 are some of the largest periodic windows in the dynamics of the drive. The driving of the Duffing system, Eq. (5) by varying c takes the dynamics of the response into different dynamical regimes of GS and at sufficiently high values of c, regions of asynchrony is

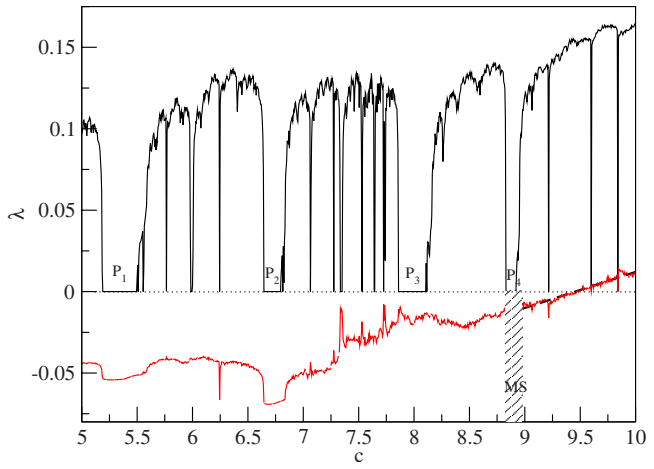

FIG. 2. (Color online) Variation of Lyapunov exponents of the drive Eq. (3) (black) and response Eq. (5) [red (dark gray)] along the line $h=0.2$. MS indicates a small window of multistability, where there is more than one attractor, with different Lyapunov exponents.

reached. There is some evidence for multistability around the periodic window P_4 where states of GS and asynchrony coexist: this region is marked MS (see Fig. 2).

To study the dynamical transitions from weak to strong GS, we focus in the parameter range $c=5.18$ to 5.19 around the region P_1. Figure 3(a) shows the variation of the largest Lyapunov exponent λ_d of the drive as a function of this parameter. The dynamics is chaotic for $c \leq c_I \approx 5.185\,05$ (marked by the arrow), with an abrupt transition to a limit

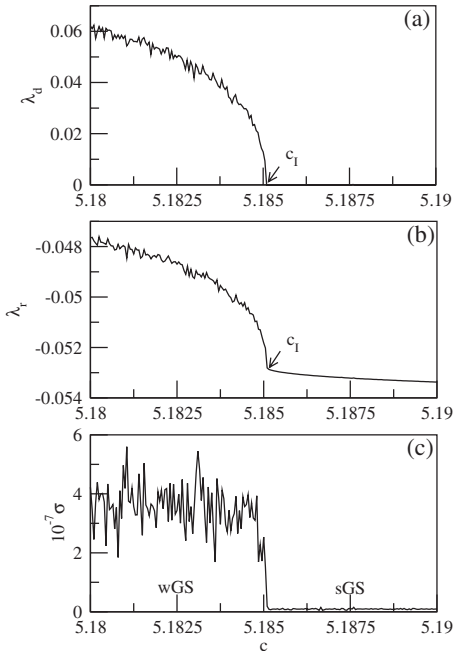

FIG. 3. The largest Lyapunov exponent (a) λ_d of the driving Rössler oscillator Eq. (3) and (b) λ_r of response Duffing oscillator Eq. (5). (c) Variance of λ_r evaluated from ensembles of initial conditions. In (c) wGS and sGS corresponds to regime of weak and strong generalized synchronization, and c_I indicates the bifurcation point in the drive and response systems, respectively.

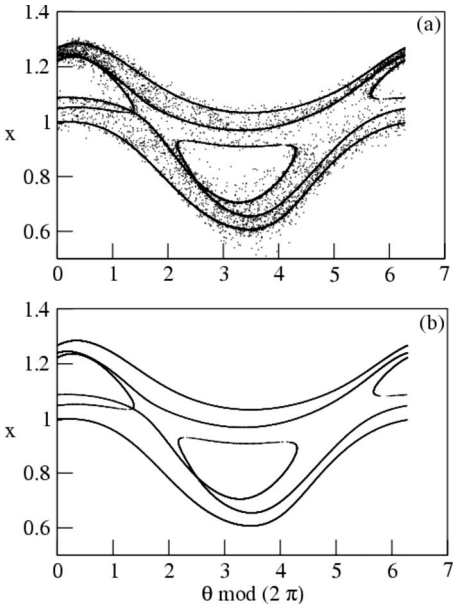

FIG. 4. Projection of the dynamics of the response Duffing oscillator Eq. (5) on Poincaré section of $(x,\theta \bmod 2\pi)$ plane. (a) Intermittent limit set at $c=5.185$ in the regime of weak GS. (b) Smooth limit set $c=5.1851$ in the regime of strong GS.

cycle for $c > c_I$. The response dynamics of the Duffing oscillator Eq. (5) is nonchaotic throughout this range, see Fig. 3(b). However at $c=c_I$, the Lyapunov exponent λ_r decreases sharply while beyond this point it decreases slowly.

The intermittency transition in the drive induces intermittency in the response as well. Shown in Fig. 4(a) is the Poincaré section for an orbit in the (x,θ) plane [19]: the limit set is nonsmooth and dynamics on it is both intermittent and nonchaotic. A regime of weak generalized synchronization is manifest [7]. Below c_I the dynamics is characterized by intermittency. Upon increasing c above c_I, a regime of strong GS results; the limit set becomes smooth as shown in Fig. 4(b). Similar dynamical transitions of GS are also observed inside P_2 window in Fig. 2.

The dynamical transitions from weak GS to strong GS can also be detected in the behavior of variance of the finite-time Lyapunov exponents. Shown in Fig. 3(c) is the variance of the response finite-time Lyapunov exponents. In general at this intermittency transition both the Lyapunov exponents and the variance show abrupt changes, with power–law variation [19–21].

B. Blowout

In systems possessing a symmetric invariant subspace, the destabilization of this subspace by variation of a system parameter results in the so-called "on-off intermittency" at a blowout bifurcation. A well-studied model in this context is the nonlinear oscillator [24,23]

$$\ddot{x} + \kappa\dot{x} + \eta x^3 + [\mu + f_1(t) + f_2(t)]\sin(2\pi x) = 0, \qquad (6)$$

where $f_i(t), i=1,2$ are arbitrary time-dependent functions, and the invariant subspace is the point $x=0,\ \dot{x}=0$.

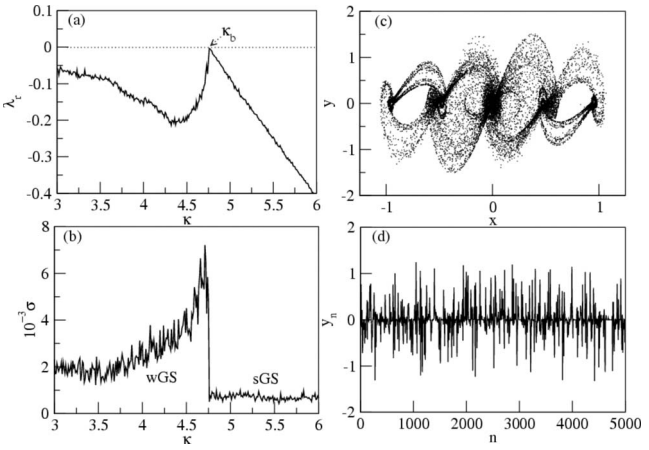

FIG. 5. Variation of (a) Lyapunov exponent λ_r of response Eq. (7) (b) Variance of Lyapunov exponents λ_r with κ (κ_b is the point of blowout bifurcation). (c) Projection of trajectory on the stroboscopic section at $\kappa=4.5$ showing a nonsmooth limit set. (d) Trajectory of y_n on the nonsmooth limit set showing on-off intermittency.

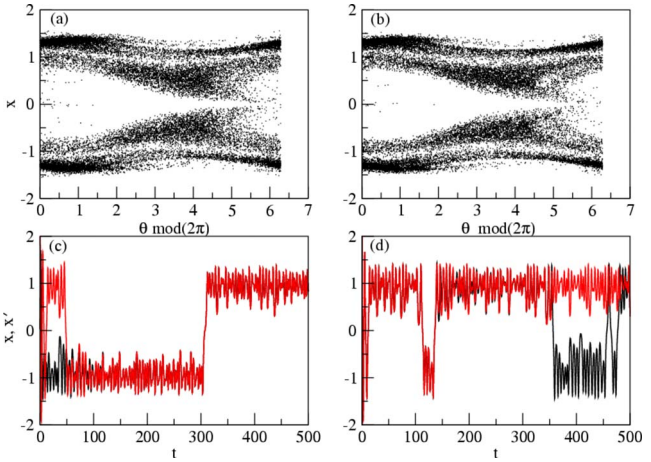

FIG. 6. (Color online) Strange limit sets of the forced Duffing oscillator, Eq. (5) in the regime of (a) weak GS at $c=9.2(\lambda_r \approx -0.0068)$ and (b) asynchrony at $c=9.79(\lambda_r \approx 0.0066)$. (c) Trajectories at $c=9.2$ (weak GS) starting from different initial conditions synchronize after some initial transients. (d) At $c=9.79$ (asynchrony), two nearby trajectories get desynchronize.

We take one forcing function to be harmonic, and the second to be the Rössler drive, rewriting the system as follows:

$$\dot{x} = y,$$

$$\dot{y} = -\kappa y - \eta x^3 + (\mu + \sin\theta + u)\sin(2\pi x),$$

$$\dot{\theta} = 1. \tag{7}$$

Here κ, η, and μ are parameters of the response, and the chaotic signal $u(t)$ is the output of the Rössler oscillator with $a=b=0.2$, $c=5.7$, and $f=1$.

The largest Lyapunov exponent of the response, λ_r of Eq. (7) from an ensemble of initial conditions with $\eta=2$ and $\mu=-1.1$ is computed as a function of κ. As can be seen in Fig. 5(a), when κ decreases, λ_r increases sharply to zero at $\kappa_b \approx 4.76$, and then decreases, showing the blowout bifurcation in the response dynamics. Thus in the entire range, the response system is in generalized synchrony with the drive: strong GS for $\kappa > \kappa_b$ and weak GS for $\kappa \leq \kappa_b$. This abrupt change in the nature of the synchronization is evident in the behavior of the variance of finite-time Lyapunov exponents. In Fig. 5(b), with decrease in κ, a sudden increase in the variance is observed at the bifurcation, signifying the destabilization of the invariant subspace, and this results in a nonsmooth limit set as shown in Fig. 5(c) (this is a stroboscopic section of a trajectory at $\theta=2\pi n$, $n=1,2\ldots$). A typical trajectory on the invariant set is transversely unstable, and exhibits on-off intermittency [25]; see Fig. 5(d) for the case of $\kappa=4.5$.

III. FROM WEAK GS TO ASYNCHRONY

When system parameters are varied the subsystem Lyapunov exponents in the coupled systems need not remain nonpositive. There is a loss of generalized synchronization when the largest of the subsystem Lyapunov exponents becomes positive: the dynamics becomes asynchronous. We examine the behavior of the largest conditional Lyapunov exponent at the transition from weak GS to asynchrony since it is known that in unforced systems, along any route to chaos, the maximal Lyapunov exponent has a characteristic signature at the transition [26–28].

The transition from nonchaotic to chaotic dynamics in forced systems has also been analyzed earlier [29], and it appears that the arguments and reasoning that was used in the study of this transition in quasiperiodically forced systems may be more generally applicable. Following the reasoning outlined in [29], we can argue that a linear variation of Lyapunov exponents will be seen in the case of chaotic forcing. Suppose a transitions from weak GS to asynchrony takes place at a critical value of drive parameter $\beta=\beta_c$ without any abrupt changes in the geometrical structure of the limit sets. A trajectory can visit both the expanding and contracting region of the phase space. Let $\lambda_e(\beta)$ and $\lambda_c(\beta)$ be the average expansion and contraction rate of a trajectory visiting the regions of synchrony and asynchrony with frequencies $f_e(\beta)$ and $f_c(\beta)$, respectively. The terms $f_e(\beta)\lambda_e(\beta)$ and $f_c(\beta)\lambda_c(\beta)$ gives the average expansion rate and contraction rate respectively. So, the Lyapunov exponent λ_r of the response which determine the average rate of expansion or contraction can be written as

$$\lambda_r(\beta) = f_e(\beta)\lambda_e(\beta) - f_c(\beta)\lambda_c(\beta). \tag{8}$$

Figure 6(a) and 6(b) shows the essentially indistinguishable limit sets of forced Duffing Eq. (5) in regions of synchrony and asynchrony, respectively. Although, morphologically both limit sets are strange or nonsmooth without any distinctive changes across the transition, but due to global stability in weak GS regime, trajectories in the same basin of attraction synchronize whereas asynchronous motion takes place when global stability is lost. Figure 6(c) and 6(d) show tra-

jectories contrasting the case of weak generalized synchrony and asynchrony phase.

In such scenarios where phase-space structure does not change drastically, one can assume that the dynamical quantities defined in this region, i.e., $\lambda_e(\beta)$, $\lambda_c(\beta)$, $f_e(\beta)$, and $f_c(\beta)$ are smooth functions of β. Taylor expansion around the transition point $\beta=\beta_c$ gives

$$\lambda_r(\beta) \approx A(\beta_c)(\beta - \beta_c) + B(\beta_c), \tag{9}$$

where $A(\beta_c)$ and $B(\beta_c)$ are slope and intercept of the line passing approximately linear from weak GS to regions of synchrony. Although there are small fluctuations in the behavior of Lyapunov exponents (which arise due to initial condition dependence in numerical computation of LE over finite interval of time), as in the case of SNAs [29], the Lyapunov exponent λ_r crosses zero approximately linearly, and with slope ≈ 0.025; this can be seen in Fig. 2 (dotted line).

IV. CHARACTERIZING STRANGENESS: PARAMETER SENSITIVITY

Although the behavior of the variance of the distribution of finite-time Lyapunov exponents (FTLEs) can detect the dynamical transition from strong to weak GS, it does not give much information about the geometry of the limit sets. The nature of this geometry, in particular the degree of "strangeness" can be determined by analyzing the sensitivity of the dynamics to perturbations of external forcing [30] or of the system parameters [31].

The sensitivity of the response $\mathbf{x}$ to perturbations of the drive initial conditions, namely $\partial\mathbf{x}/\partial\mathbf{u}_0$ gives a good measure for quasiperiodically forced systems [30]. This does not appear to be useful for other types of forcing. To see this, for $\mathbf{u} \in \mathbb{R}$, by differentiating Eq. (1) with respect to the drive variable, one gets

$$\frac{d}{dt}\frac{\partial \mathbf{x}}{\partial u_0} = \sum_{j=1}^{n} \frac{\partial F}{\partial x_j}\frac{\partial x_j}{\partial u_0} + \frac{\partial F}{\partial u}\frac{\partial u}{\partial u_0}. \tag{10}$$

Note that in the last term, $\partial u/\partial u_0$ is determined by the stability characteristics of the drive: for quasiperiodic forcing, $\partial u/\partial u_0 = 1$ and thus $\partial\mathbf{x}/\partial u_0$ which is obtained by integrating Eq. (10) is a good measure to quantify the strangeness of the limit sets [30]: $|\partial\mathbf{x}/\partial u_0|$ is bounded for smooth limit sets, whereas it is unbounded for nonsmooth limit sets. However, if $\partial u/\partial u_0 \neq 1$ the situation is less clear.

In such cases, the parameter sensitivity [31,32] provides a good measure to characterize dynamical transitions associated with a change in the morphology of the invariant set. Adapting the parameter sensitivity analysis for the present case of time continuous systems, note that upon differentiating Eq. (1) with respect to system parameter α, one gets

$$\frac{d}{dt}\frac{\partial \mathbf{x}}{\partial \alpha} = \sum_{j=1}^{n} \left(\frac{\partial F}{\partial x_j}\right)_{\alpha} \left(\frac{\partial x_j}{\partial \alpha}\right)_{x} + \left(\frac{\partial F}{\partial \alpha}\right)_{x}, \tag{11}$$

which can be solved to obtain $\partial\mathbf{x}/\partial\alpha$, the sensitivity of response with respect to a system parameter. Depending on the dynamics of the response, the quantity

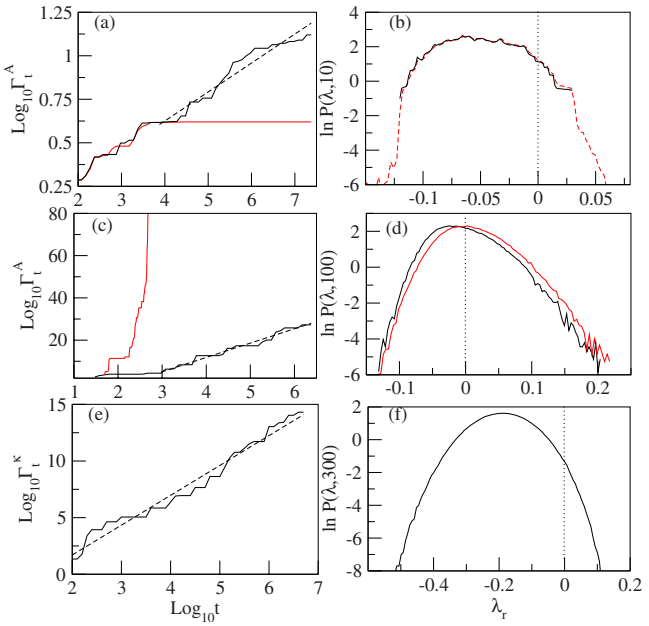

FIG. 7. (Color online) Parameter sensitivity exponents (left panel) and corresponding distribution of finite-time Lyapunov exponents (FTLEs) (right panel) of response dynamics for Eq. (5) in (a)–(d) and Eq. (7) in (e) and (f): (a) Strong GS [red (dark gray) line] and weak GS (black line); (b) strong GS (black line) and weak GS [red (dark gray)] line; (c) asynchrony [red (dark gray) line] and weak GS (black line); (d) asynchrony [red (dark gray) line] and weak GS (black line); (e) weak GS due to blowout bifurcation and its (f) FTLEs distribution.

$$\gamma = \max_{0\le k\le t}\left|\frac{\partial \mathbf{x}_k}{\partial \alpha}\right|, \tag{12}$$

namely, the upper envelope of the signal $\partial\mathbf{x}_k/\partial\alpha$ has three typical behaviors.

When the largest of the subsystem Lyapunov exponents is positive, $\gamma \sim \exp(\lambda_r t)$ because of exponential divergence of the orbits. This corresponds to a lack of generalized synchronization. In regions of generalized synchrony where the largest exponent is nonpositive, it can be shown that $\gamma \sim t^{\mu}$ with exponents $\mu=0$ for regular dynamics, namely, for the case of strong GS, and $\mu \neq 0$ for irregular dynamics, namely for the case of weak GS.

Another suitably averaged quantity to consider is the lower envelope of different γ_s of different initial conditions,

$$\Gamma_t = \min_{x_0,u_0}\{\gamma\} \tag{13}$$

and this proves to be more appropriate to use for characterization of the limit sets. In the region of nonchaotic dynamics, again

$$\Gamma_t \sim t^{\mu} \tag{14}$$

and the exponent μ is a good measure for characterization of the dynamics and the "degree of strangeness."

Figure 7(a) shows parameter sensitivity of the dynamics across the intermittent transition from weak to strong GS in the forced Duffing system. The sensitivity exponent (black

line) for intermittent dynamics in regime of weak GS at $c=5.185$ grows with $\mu \approx 0.166$ whereas it [red (dark gray) line] saturates for dynamics in regime of strong GS at $c=5.1851$. This behavior can be contrasted with the distributions of finite-time Lyapunov exponents (FTLEs) [33] which is defined as

$$P(\lambda_r,t)d\lambda_r = \text{Probability that } \lambda_r(t) \text{ takes a value between } \lambda_r(t) \text{ and } \lambda_r(t)+d\lambda_r(t). \quad (15)$$

Figure 7(b) shows the distributions of FTLEs of the forced Duffing oscillator evaluated for trajectory length $t=10$. At $c=5.1851$ for the case of strong GS, the distribution of FTLEs (solid line) is largely confined to the negative axis, whereas FLTEs for the intermittent weak GS at $c=5.185$ (dashed line) extends into the positive axis [34,35]. Figure 7(c) and 7(d) shows the dynamical difference between the regime of weak GS and asynchrony. The behavior of parameter sensitivity across the transition from weak GS to asynchrony is shown in Fig. 7(c). At the regime of weak GS at $c=9.2$, there is a power law growth (black line) with exponent ($\mu \approx 6.782$) but the behavior changes to exponential [red (dark gray) line] in regime of asynchrony at $c=9.79$. In Fig. 7(d), the distribution of FTLEs across the transitions is shown: The mean of distribution shifts toward the positive components as one approach regions of asynchrony [red (dark gray) line] from weak GS (black line).

Shown in Fig. 7(e) and 7(f) are the corresponding quantities at the blowout transition in the forced systems, Eq. (7). The parameter sensitivity of the dynamics for weak GS in this system at $\kappa=4.5$ has power law growth with exponent $\mu \approx 2.636$, while the distribution of FTLEs for trajectory length $t=300$ is Gaussian; see Fig. 7(f).

V. SUMMARY AND DISCUSSION

External driving of nonlinear dynamical systems can give rise to a stable response that is in a state of generalized synchronization with the drive. In the present work we have studied the structure of this state by examining the so-called strong and weak forms of generalized synchronization, the transition between them, and the loss of synchronization when system parameters are varied.

Our strategy has been to exploit the parallels between strange nonchaotic motion and weak generalized synchronization [7]. We have examined two specific "routes," the intermittency and blowout bifurcation transition from strong to weak GS in *driven flows*, and show that the parameter sensitivity provides a good measure to detect the dynamical transition from weak GS to strong GS since this is sensitive to the degree of strangeness of the limit set on which generalized synchronization occurs. At the transition from weak GS to asynchronous dynamics, as in the case of the SNAs to chaotic attractor transition [29], the Lyapunov exponent varies linearly as it crosses zero. This similarity further underscores the fact that SNAs should be viewed as a manifestation of weak GS [7].

A major motivation that has governed our choice of the driven nonlinear dynamical system has been that the phenomena that are described should be experimentally realizable. Therefore we have examined the Duffing oscillator, Eq. (5) as a model response system. An experimental system that is closely modeled by this oscillator is the magnetoelastic ribbon which has been earlier studied under the effect of quasiperiodic driving [36]. The second system we studied, Eq. (7), corresponds to a driven superconducting quantum interference device (SQUID) [24]. Thus we believe that the transitions discussed here can, in principle, be detected in laboratory experiments.

Chaotic motion—and therefore chaotic modulation—is widespread in natural systems. As a consequence, the occurrence of generalized synchrony may well be the most robust mechanism for the creation of temporal correlations in nature, given the fact that nonlinearity and coupling are both common features of natural systems. Indeed, stabilization of dynamics by quasiperiodic forcing has been suggested as a mechanism that neural systems could exploit [37,38], although it is not easy to identify a reliable source of quasiperiodicity in nature. Given the ubiquity of stochasticity and chaos in biological systems over a wide range of time scales [37,39,40,15,41], the stability of such dynamics may be the result of generalized synchronization to a chaotic environment.

ACKNOWLEDGMENTS

We thank Awadhesh Prasad for discussions and acknowledge the CSIR, India for support of T.U.S and H.H.J.

[1] A. Pikovsky, M. Rosenblum, and J. Kurths, *Synchronization: A Universal Concept in Nonlinear Sciences* (Cambridge University Press, Cambridge, England, 2001).
[2] L. M. Pecora and T. L. Carroll, Phys. Rev. Lett. **64**, 821 (1990).
[3] C. Grebogi, E. Ott, S. Pelikan, and J. Yorke, Physica D **13**, 261 (1984).
[4] N. F. Rulkov, M. M. Sushchik, L. S. Tsimring, and H. D. I. Abarbanel, Phys. Rev. E **51**, 980 (1995); L. Kocarev and U. Parlitz, Phys. Rev. Lett. **76**, 1816 (1996).
[5] K. Pyragas, Phys. Rev. E **54**, R4508 (1996).
[6] B. R. Hunt, E. Ott, and J. A. Yorke, Phys. Rev. E **55**, 4029 (1997).
[7] T. U. Singh, A. Nandi, and R. Ramaswamy, Phys. Rev. E **78**, 025205(R) (2008).
[8] J. P. Eckmann and D. Ruelle, Rev. Mod. Phys. **57**, 617 (1985).
[9] A. Prasad, S. S. Negi, and R. Ramaswamy, Int. J. Bifurcat. Chaos **11**, 291 (2001).
[10] J. Stark and M. E. Davies, IEE Digest **143**, 1 (1994).
[11] S. Ljung and L. Ljung, Automatica **21**, 157 (1985).
[12] R. Badii, G. Broggi, B. Derighetti, M. Ravani, S. Ciliberto, A. Politi, and M. A. Rubio, Phys. Rev. Lett. **60**, 979 (1988).

[13] C. S. Zhou and T. L. Chen, Europhys. Lett. **38**, 261 (1997).
[14] K. M. Cuomo and A. V. Oppenheim, Phys. Rev. Lett. **71**, 65 (1993).
[15] L. Glass, Nature (London) **410**, 277 (2001).
[16] S. J. Schiff, P. So, T. Chang, R. E. Burke, and T. Sauer, Phys. Rev. E **54**, 6708 (1996).
[17] B. Blasius, A. Huppert, and L. Stone, Nature (London) **399**, 354 (1999).
[18] J. P. Loy and C. R. Weiss, Econ. Lett. **85**, 123 (2004).
[19] J. Heagy and W. L. Ditto, J. Nonlinear Sci. **1**, 423 (1991).
[20] A. Prasad, V. Mehra, and R. Ramaswamy, Phys. Rev. Lett. **79**, 4127 (1997).
[21] A. Venkatesan, M. Lakshmanan, A. Prasad, and R. Ramaswamy, Phys. Rev. E **61**, 3641 (2000).
[22] T. U. Singh, Ph.D. thesis, Jawaharlal Nehru University, 2010.
[23] T. Yalçinkaya and Y. C. Lai, Phys. Rev. Lett. **77**, 5039 (1996).
[24] T. Zhou, F. Moss, and A. Bulsara, Phys. Rev. A **45**, 5394 (1992).
[25] J. C. Sommerer and E. Ott, Phys. Lett. A **188**, 39 (1994).
[26] Y. Pomeau and P. Manneville, Commun. Math. Phys. **74**, 189 (1980).
[27] M. J. Feigenbaum, J. Stat. Phys. **19**, 25 (1978).
[28] C. Grebogi, E. Ott, and J. A. Yorke, Phys. Rev. Lett. **48**, 1507 (1982).
[29] Y.-C. Lai, Phys. Rev. E **53**, 57 (1996).
[30] A. S. Pikovsky and U. Feudel, Chaos **5**, 253 (1995).
[31] T. Nishikawa and K. Kaneko, Phys. Rev. E **54**, 6114 (1996).
[32] A. Jalnine and S. Y. Kim, Phys. Rev. E **65**, 026210 (2002).
[33] H. D. I. Abarbanel, R. Brown, and M. B. Kennel, J. Nonlinear Sci. **2**, 343 (1992).
[34] A. Prasad and R. Ramaswamy, Phys. Rev. E **60**, 2761 (1999).
[35] S. Datta and R. Ramaswamy, J. Stat. Phys. **113**, 283 (2003).
[36] W. L. Ditto, M. L. Spano, H. T. Savage, S. N. Rauseo, J. Heagy, and E. Ott, Phys. Rev. Lett. **65**, 533 (1990).
[37] A. J. Mandell and K. A. Selz, J. Stat. Phys. **70**, 355 (1993).
[38] A. Prasad, B. Biswal, and R. Ramaswamy, Phys. Rev. E **68**, 037201 (2003).
[39] M. I. Rabinovich and H. D. I. Abarbanel, Neuroscience **87**, 5 (1998).
[40] Z. R. Struzik, K. Kiyono, J. Hayano, E. Watanabe, and Y. Yamamoto, Europhys. Lett. **82**, 28005 (2008).
[41] M. Kærn *et al.*, Nat. Rev. Genet. **6**, 451 (2005).